# EQUATIONS OF STATE FOR N-HEXADECANE AND N-DOCOSANE

Raffaella Romeo[1]*, Eric W. Lemmon[2]

[1] Istituto Nazionale di Ricerca Metrologica, Strada delle Cacce 91, Turin, Italy

[2] Applied Chemicals and Materials Division, National Institute of Standards and Technology, 325 Broadway, Boulder, Colorado 80305, USA

*Corresponding author: Raffaella Romeo r.romeo@inrim.it

Keywords: equations of state, *n*-hexadecane, *n*-docosane, Helmholtz energy, thermodynamic properties

## ABSTRACT

Equations of state for *n*-hexadecane ($C_{16}H_{34}$) and *n*-docosane ($C_{22}H_{46}$) have been developed as functions of the Helmholtz energy with independent variables of temperature and density. The equations were developed based on experimental values of density, speed of sound, isobaric heat capacity, and vapor pressure. With these equations, all thermodynamic properties of *n*-hexadecane and *n*-docosane can be calculated. For *n*-hexadecane, the uncertainty in vapor pressure is 0.5%. The uncertainty of the saturated liquid density is 0.05% from the triple point up to 400 K, and 0.2% at higher temperatures. The uncertainty in densities is within 0.5%. The speed of sound and isobaric heat capacity can be calculated within 0.25%. The uncertainties of the properties calculated with the equation for *n*-docosane are 5% for vapor pressure, 0.1% for saturated liquid density, 1% for density, 0.5% and 1% for speed of sound at atmospheric pressure and higher pressures, respectively, and within 3% for heat capacity.

## INTRODUCTION

*n*-Hexadecane ($C_{16}H_{34}$) and *n*-docosane ($C_{22}H_{46}$) are normal alkanes of interest in the petroleum industry for multiple applications. They are generally used as constituents in mixtures for fuel, especially for aviation. In this work, fundamental equations of state, in terms of the Helmholtz energy, are presented for both liquids. The equations of state are valid over the whole fluid region, and through them all thermodynamic properties can be calculated. Measurements of vapor pressure, density, speed of sound, and heat capacity are available in the literature for both *n*-hexadecane and *n*-docosane. Although the amount of data available for *n*-hexadecane is quite large, *n*-docosane is less studied, as with other heavy alkanes. The experimental data (reported in references 1-84) were used to develop the equations of state and estimate their uncertainties.

## CRITICAL AND TRIPLE POINT VALUES

The critical values are among the most important parameters in the development of equations of state, such as for use as the reducing parameters in the equations. In the work of Lemmon and Goodwin [85], equations for the critical temperatures and pressures of normal alkanes, as functions of the carbon

number, were determined. In the present work, the critical temperature values calculated by Lemmon and Goodwin were adopted for both fluids; the critical densities $\rho_c$ were determined during the fitting process of the equations of state. The critical pressures $p_c$ were calculated from the final equations of state as a fixed point at the critical temperature and density.
The values of the critical point determined in this work for *n*-hexadecane are

$$T_c = 722.1 \text{ K}$$

$$p_c = 1.4799 \text{ MPa}$$

$$\rho_c = 1.000 \text{ mol·dm}^{-3}$$

The triple point temperature of *n*-hexadecane is 291.329 K, and its molar mass is 226.441 g·mol$^{-1}$ [86].

The critical values of *n*-docosane are

$$T_c = 792.2 \text{ K}$$

$$p_c = 1.1740 \text{ MPa}$$

$$\rho_c = 0.723 \text{ mol·dm}^{-3}$$

The triple point temperature of *n*-docosane is 587.6 K and its molar mass is 310.601 g·mol$^{-1}$ [86].

ANCILLARY EQUATIONS

The boundaries between the liquid and vapor phases are defined by saturation states that can be estimated through the use of ancillary equations. These give close estimates for the pressures and densities required in the iterative process to find the saturation states. The ancillary equations were developed by fitting calculated values of the saturation states (determined with the application of the Maxwell criteria applied to the equations of state) [87].

**Ancillary equations for *n*-hexadecane**

The ancillary form for the vapor pressure $p_\sigma$ is

$$\ln\left(\frac{p_\sigma}{p_c}\right) = \frac{T_c}{T}\left[N_1\theta + N_2\theta^{1.5} + N_3\theta^{2.8} + N_4\theta^{6.7} + N_5\theta^{8.9} + N_6\theta^{15.5}\right] \quad (1)$$

where $\theta = 1 - \frac{T}{T_c}$, $N_1$= −10.4856, $N_2$ = 3.8226, $N_3$ = −8.6727, $N_4$ = −4.1440, $N_5$ = 0.8801, and $N_6$ = −5.7224.

The saturated liquid density $\rho'$ can be calculated by the following ancillary equation

$$\frac{\rho'}{\rho_c} = 1 + N_1\theta^{0.39} + N_2\theta^{0.84} + N_3\theta^{1.27} + N_4\theta^{1.72} + N_5\theta^{2.26} \quad (2)$$

where $N_1$= 3.43, $N_2$ = −4.008, $N_3$ = 8.4779, $N_4$ = −7.894, and $N_5$ = 3.4824.

The ancillary equation that represents the saturated vapor density $\rho''$ is

$$\ln\left(\frac{\rho''}{\rho_c}\right) = N_1\theta^{0.44} + N_2\theta^{2.32} + N_3\theta^{1.75} + N_4\theta^{4.4} + N_5\theta^{9.97} + N_6\theta^{20.9} \quad (3)$$

where $N_1$ = −5.0096, $N_2$ = 0.9061, $N_3$ = −15.2865, $N_4$ = −61.4138, $N_5$ = −143.5222, and $N_6$ = −369.0229.

**Ancillary equations for *n*-docosane**

The ancillary form representing the vapor pressure $p_\sigma$ is

$$\ln\left(\frac{p_\sigma}{p_c}\right) = \frac{T_c}{T}[N_1\theta + N_2\theta^{1.5} + N_3\theta^{2.7} + N_4\theta^{5.5} + N_5\theta^{14.1} + N_6\theta^{52.1}] \quad (4)$$

where $N_1$ = −12.3834, $N_2$ = 2.8818, $N_3$ = −11.6292, $N_4$ = −2.7357, $N_5$ = −7.3103, and $N_6$ = 1188.9117.
The saturated liquid density $\rho'$ can be calculated with

$$\frac{\rho'}{\rho_c} = 1 + N_1\theta^{0.5} + N_2\theta^{0.8} + N_3\theta^{1.2} + N_4\theta^{1.8} + N_5\theta^{2.5} \quad (5)$$

where $N_1$ = 6.6254, $N_2$ = −11.0123, $N_3$ = 13.6452, $N_4$ = −8.8244, and $N_5$ = 3.1241.

The ancillary equation that represents the saturated vapor density $\rho''$ is

$$\ln\left(\frac{\rho''}{\rho_c}\right) = N_1\theta^{0.5} + N_2\theta^{24.0} + N_3\theta^{1.7} + N_4\theta^{4.2} + N_5\theta^{10.3} + N_6\theta^{10.6} \quad (6)$$

where $N_1$ = −5.9790, $N_2$ = −586.6421, $N_3$ = −14.3725, $N_4$ = −71.0676, $N_5$ = −213.3123, and $N_6$ = 15.7901.

EQUATION OF STATE

The form of the equation of state presented in this work is based on the Helmholtz energy as a function of density and temperature $a(\rho,T)$, which is the most commonly used form for the calculation of thermodynamic properties of pure fluids and mixtures with low uncertainties. All thermodynamic properties can be estimated as derivatives of the Helmholtz energy, for example, pressure is calculated as

$$p = \rho^2\left(\frac{\partial a}{\partial \rho}\right)_T. \quad (7)$$

The derivatives of the Helmholtz energy required to calculate other thermodynamic properties not reported are given elsewhere, e.g. [88].

The functional form for the reduced Helmholtz energy $\alpha$, as a function of the dimensionless density and temperature, is

$$\frac{a(\rho,T)}{RT} = \alpha(\delta,\tau) = \alpha^0(\delta,\tau) + \alpha^r(\delta,\tau) \quad (8)$$

where $\delta = \rho/\rho_c$, $\tau = T_c/T$, and $R$ is the molar gas constant equal to 8.314462618 J·mol$^{-1}$·K$^{-1}$ [89].

The reduced Helmholtz energy $\alpha$ is the contribution from the ideal gas contribution $\alpha^0$, which represents the ideal gas properties, and the residual or real Helmholtz energy $\alpha^r$ that accounts for the interactions between molecules.

**Properties of the ideal gas**

The ideal gas Helmholtz energy has the following form [90]:

$$\alpha^0 = \ln\delta + (c_0 - 1)\ln\tau + \sum_{k=1}^{2} a_k \tau^{i_k} + \sum_{k=1}^{2} v_k \ln\left[1 - e^{\frac{-u_k \tau}{T_c}}\right] \tag{9}$$

where the coefficients for *n*-hexadecane and *n*-docosane are given in Tables 1 and 2, respectively.

In order to calculate thermodynamics properties, a model for the ideal gas isobaric heat capacity is necessary. The expression for the ideal gas isobaric heat capacity $c_p^0$ used in this work that is required to derive the ideal gas Helmholtz energy is

$$\frac{c_p^0}{R} = c_0 + \sum_{k=1}^{2} v_k \left(\frac{u_k}{T}\right)^2 \frac{e^{u_k/T}}{[e^{u_k/T} - 1]^2} \tag{10}$$

The $u_k$ coefficients contained in the Einstein functions used in this equation give the proper shape of the ideal gas heat capacity similar to that derived from statistical mechanical models.
The values of $a_k$, $v_k$, and $u_k$ are given in Table 1 for *n*-hexadecane and in Table 2 for *n*-docosane.

Table 1. Coefficients and exponents of the ideal gas Helmholtz energy equation for *n*-hexadecane.

| $c_0$ | $k$ | $a_k$ | $i_k$ | $v_k$ | $u_k$ |
|---|---|---|---|---|---|
| 23.03 | 1 | 45.96 | 0 | 18.91 | 420 |
| | 2 | −26.19 | 1 | 76.23 | 1860 |

Table 2. Coefficients and exponents of the ideal gas Helmholtz energy equation for *n*-docosane.

| $c_0$ | $k$ | $a_k$ | $i_k$ | $v_k$ | $u_k$ |
|---|---|---|---|---|---|
| 33.9 | 1 | 66.73 | 0 | 61.6 | 1000 |
| | 2 | −44.17 | 1 | 77.7 | 2400 |

**Properties of the real gas**

The functional form often used till about the year 2000 for the residual Helmholtz energy equation was

$$\alpha^{\mathrm{r}}(\delta,\tau) = \sum N_k \delta^{d_k} \tau^{t_k} + \sum N_k \delta^{d_k} \tau^{t_k} \exp\left(-\delta^{l_k}\right). \tag{11}$$

A form containing additional Gaussian bell-shaped terms is now typically used, including those for *n*-hexadecane and *n*-docosane in this work, and is expressed as

$$\alpha^{\mathrm{r}}(\delta,\tau) = \sum_{k=1}^{k_1} N_k \delta^{d_k} \tau^{t_k} + \sum_{k=k_1+1}^{k_2} N_k \delta^{d_k} \tau^{t_k} \exp\left[-\delta^{l_k}\right] + \sum_{k=k_2+1}^{k_3} N_k \delta^{d_k} \tau^{t_k} \exp[-\eta_k(\delta-\epsilon_k)^2 - \beta_k(\tau-\gamma_k)^2] \tag{12}$$

where the coefficients and exponents are reported in Table 3 for *n*-hexadecane and in Table 4 for *n*-docosane and the values of $k_1$, $k_2$, and $k_3$ for the equations in this work are 5, 10, and 15. The Gaussian terms are useful in the determination of the fluid properties in the critical range.

Table 3. Coefficients of the equation of state for *n*-hexadecane; coefficients not listed are zero.

| $k$ | $N_k$ | $t_k$ | $d_k$ | $l_k$ | $\eta_k$ | $\beta_k$ | $\gamma_k$ | $\varepsilon_k$ |
|---|---|---|---|---|---|---|---|---|
| 1 | 0.03965879 | 1 | 4 | | | | | |
| 2 | 1.945813 | 0.224 | 1 | | | | | |
| 3 | −3.738575 | 0.91 | 1 | | | | | |
| 4 | −0.342167 | 0.95 | 2 | | | | | |
| 5 | 0.3427022 | 0.555 | 3 | | | | | |
| 6 | −2.519592 | 2.36 | 1 | 2 | | | | |
| 7 | −0.8948857 | 3.58 | 3 | 2 | | | | |
| 8 | 0.10760773 | 0.5 | 2 | 1 | | | | |
| 9 | −1.297826 | 1.72 | 2 | 2 | | | | |
| 10 | −0.048332312 | 1.078 | 7 | 1 | | | | |
| 11 | 4.245522 | 1.14 | 1 | | 0.641 | 0.516 | 1.335 | 0.75 |
| 12 | −0.31527585 | 2.43 | 1 | | 1.008 | 0.669 | 1.187 | 1.616 |
| 13 | −0.7212941 | 1.75 | 3 | | 1.026 | 0.25 | 1.39 | 0.47 |
| 14 | −0.2680657 | 1.1 | 2 | | 1.21 | 1.33 | 1.23 | 1.306 |
| 15 | −0.7859567 | 1.08 | 2 | | 0.93 | 2.1 | 0.763 | 0.46 |

Table 4. Coefficients of the equation of state for *n*-docosane.

| $k$ | $N_k$ | $t_k$ | $d_k$ | $l_k$ | $\eta_k$ | $\beta_k$ | $\gamma_k$ | $\varepsilon_k$ |
|---|---|---|---|---|---|---|---|---|
| 1 | 0.04239455 | 1 | 4 | | | | | |
| 2 | 2.370432 | 0.224 | 1 | | | | | |
| 3 | −4.30263 | 0.91 | 1 | | | | | |
| 4 | −0.4039603 | 0.95 | 2 | | | | | |
| 5 | 0.4005704 | 0.555 | 3 | | | | | |
| 6 | −2.643419 | 2.36 | 1 | 2 | | | | |
| 7 | −0.9199641 | 3.58 | 3 | 2 | | | | |
| 8 | 0.1394402 | 0.5 | 2 | 1 | | | | |
| 9 | −1.448862 | 1.72 | 2 | 2 | | | | |
| 10 | −0.0547678 | 1.078 | 7 | 1 | | | | |
| 11 | 4.579069 | 1.14 | 1 | | 0.641 | 0.516 | 1.335 | 0.75 |
| 12 | −0.3534636 | 2.43 | 1 | | 1.008 | 0.669 | 1.187 | 1.616 |
| 13 | −0.8217892 | 1.75 | 3 | | 1.026 | 0.25 | 1.39 | 0.47 |
| 14 | −0.2604273 | 1.1 | 2 | | 1.21 | 1.33 | 1.23 | 1.306 |
| 15 | −0.7618884 | 1.08 | 2 | | 0.93 | 2.1 | 0.763 | 0.46 |

FITTING CONSTRAINTS

In order to develop the equations of state, several constraints were used to control the shape of the thermodynamic surface. In Table 5, a list of the main constraints for *n*-hexadecane is given. The table shows the properties for which a constraint was needed, the kind of constraint imposed, and the range over which it was applied. Because the thermodynamic behavior of *n*-hexadecane and *n*-docosane is, for the most part, the same when viewed on a reduced basis (such as with $\tau$ and $\delta$), the constraints used for *n*-hexadecane can be applied directly to the fitting of *n*-docosane after the temperature and density ranges of the constraints have been properly adjusted, and thus they are not reported here.

As an example, the rectilinear diameter (the average of the vapor and liquid saturated densities) was constrained to be linear by imposing zero curvature from 650 K to the critical temperature; it results in the behavior shown in Figure 1. In preliminary fits the fourth virial coefficient was negative around 1500 K to 2500 K, thus it was forced to give positive values in the temperature range between 1300 K and 3000 K, as presented in Figure 2.

The phase identification parameter (PIP) [91] required many constraints. An example is the constraint acting on the isobar at 1 MPa over the temperature range from 200 K to 420 K that forced the slope, curvature, and third and fourth derivatives to all be positive. A further constraint was used to obtain negative curvature of the isotherm at 1000 K between 1.08 mol·dm$^{-3}$ and 1.85 mol·dm$^{-3}$ (see Figure 3). More details about the phase identification parameter and the fourth virial coefficient are reported in a following section.

Table 5. Constraints for *n*-hexadecane.

| Property | Constraint | Range |
|---|---|---|
| Speed of sound | Negative slope and 3rd derivative<br>Positive curvature and 4th derivative | 1 MPa, (35 – 115) K |
| Isochoric heat capacity | Negative slope and 3rd derivative<br>Positive curvature and 4th derivative | 3 MPa, (430 – 625) K |
| Rectilinear diameter | Zero curvature | Liquid saturation line, from 650 K to $T_c$ |
| Phase identification parameter | Negative curvature | 1000 K, (1.08 – 1.85) mol·dm$^{-3}$ |
| Phase identification parameter | Zero curvature | 725 K, (0.80 – 0.95) mol·dm$^{-3}$ |
| Phase identification parameter | Positive derivatives | 1 MPa, (200 – 420) K |
| Phase identification parameter | Positive derivatives | Liquid saturation line, (580 – 650) K |
| 4th virial coefficient | Positive values | (1300 – 3000) K |
| 4th virial coefficient | Negative slope | (1000 – 1200) K |
| Ideal curve | Zero curvature | (0.02 – 2.00) mol·dm$^{-3}$ |
| Joule inversion curve | Positive curvature | (0.05 – 2.50) mol·dm$^{-3}$ |
| Joule-Thomson inv. curve | Positive curvature | (0.1 – 2.0) mol·dm$^{-3}$ |

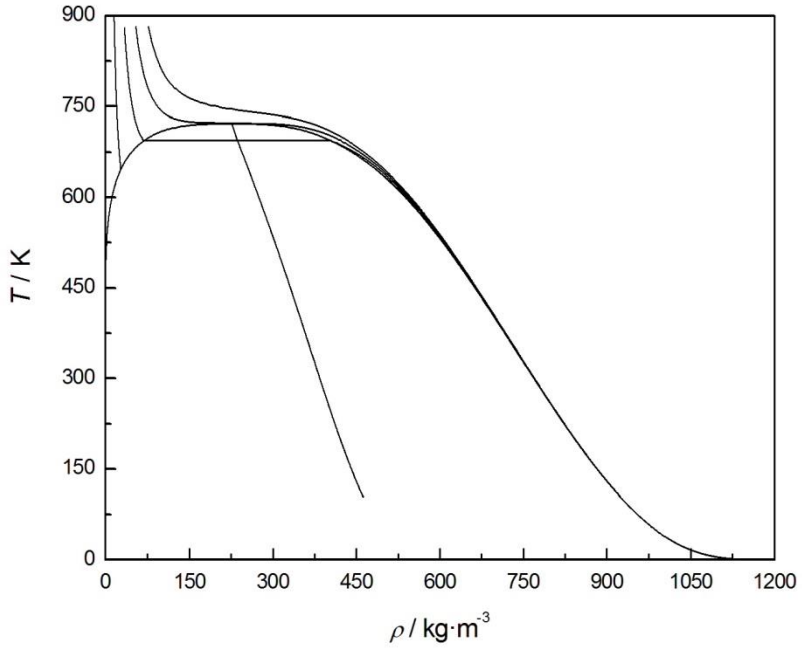


Figure 1. Temperature as a function of density for *n*-hexadecane along several isobars: the straight line is the rectilinear diameter.

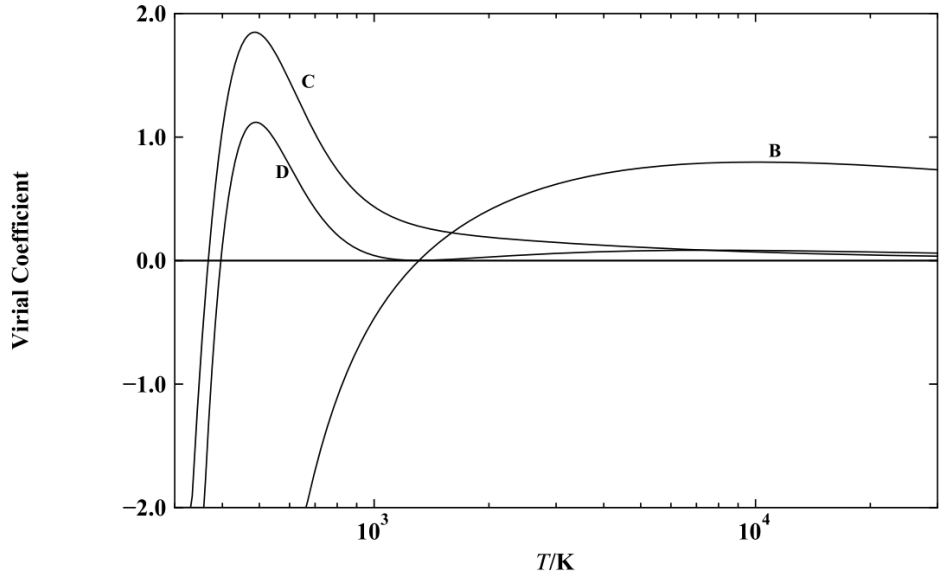


Figure 2. Virial coefficients for *n*-hexadecane, with units of $dm^3/mol$ for the second virial coefficient *B*, units of $dm^6/mol^2$ for the third virial coefficient *C*, and units of $dm^9/mol^3$ for the fourth virial coefficient *D.*

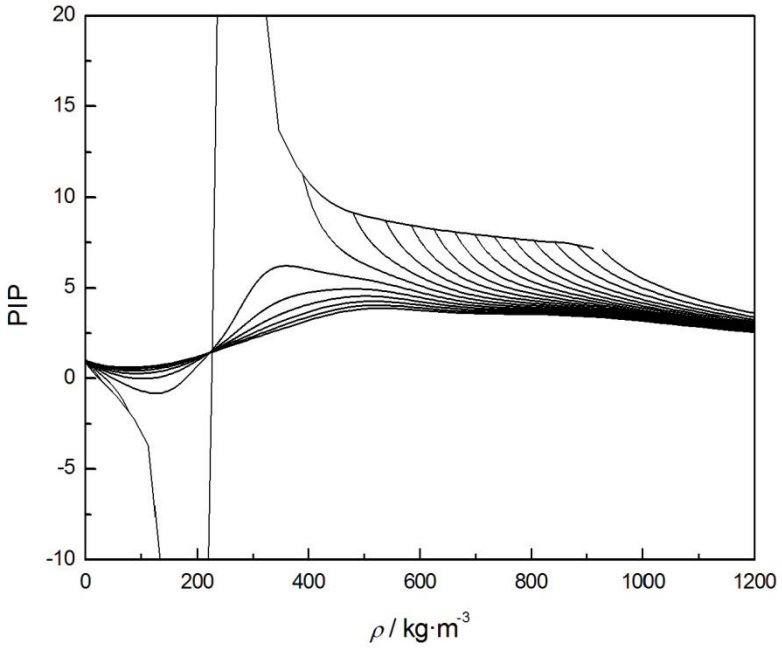


Figure 3. Phase identification parameter (PIP) as a function of density for *n*-hexadecane along isotherms from 100 K to 1000 K.

COMPARISON TO EXPERIMENTAL DATA

The experimental data used for this work are summarized in Table 6 for *n*-hexadecane and in Table 7 for *n*-docosane. The experimental data were converted to kelvins (ITS-90) for temperatures, megapascals for pressures, and moles per cubic decimeter for densities.

In order to estimate the uncertainties of the equations of state, all available experimental data are considered. The uncertainties are estimates of the combined expanded uncertainties with a coverage factor of two. The accuracy of the equations of state were determined by statistical comparisons between the properties calculated from the equations of state and the experimental values.

Tables 6 and 7 show the average absolute deviations (AAD) for any generic property *X*, as follows

$$\mathrm{AAD} = \frac{1}{n}\sum_{i=1}^{n}|\Delta X_i| \tag{13}$$

where *n* is the number of data and Δ*X* is defined as:

$$\Delta X = 100 \cdot \left(\frac{X_{\mathrm{data}} - X_{\mathrm{calc}}}{X_{\mathrm{data}}}\right) \tag{14}$$

**Comparison to *n*-hexadecane experimental data**

In Figure 4, the deviations of experimental **vapor pressures** from the equation are shown. The measurements cover a range of temperatures between 298 K and 600 K. Most of the experimental data show scatter within 2%. The data of Morgan and Kobayashi [49], Viton *et al.* [74], and Camin *et al.* [17] are best represented. The three data sets overlap between 460 K to 470 K, and the data show deviations on average within 0.1%. Above 460 K, the Morgan and Kobayashi and Camin *et al.* data agree with the equation within 0.2%. The data of Morgan and Kobayashi were carried out for temperatures up to 583 K, and the equation maintains deviations below 0.2%. For temperatures lower than 460 K, the data of Morgan and Kobayashi show deviations from the equation below 0.6%.

The deviations of **saturated liquid densities** for *n*-hexadecane are shown in Figure 5. Most of the data have deviations lower than 0.1% between 273 K and 373 K. In the temperature range between 303 K and 373 K, the data of Bolotnikov *et al.* [15], Prak *et al.* 2013 [63], and Prak *et al.* 2014 [64] show deviations lower than 0.05%. The measurements of Plebanski *et al.* [62] were performed over a wide range of temperature (from about 300 K to 490 K), with a maximum deviation of 0.07% from the equation and better than 0.02% between 340 K and 420 K.

All of the **density** data available are represented by the equation with deviations lower than about 1.5% and most are within 0.3%, as shown in Figure 6. The data of Banipal *et al.* [10] are represented by the equation within 0.1% for temperatures between 318 K and 373 K, and at pressures up to 10 MPa. At ambient pressure, the deviation is reduced to 0.05%. The deviations of the data of Snyder and Winnick [70] are below 0.1% at 298 K. Between 0.6 MPa and 28 MPa the data are within 0.1%. The measurements performed by Outcalt *et al.* [54] agree with the equation of state within 0.2%, but the deviations are consistently negative.

The deviations in **speed of sound** data from the equation are shown in Figure 7. The only available measurements at temperatures higher than 473 K are those in the work of Neruchev *et al.* [52]. The data show good agreement with the equation and are less than 0.5% for temperatures up to 693 K. At pressures between 10 MPa and 50 MPa, the data of Ball and Trusler [9], Nascimento *et al.* [51], Khasanshin and Shchemelev [39], and Boelhouwer [14] are fitted to within 0.4%. Above 50 MPa, the measurements of Boelhouwer, which were carried out up to 120 MPa, spread no more than 0.3%. For the other available data above 50 MPa (Ball and Trusler), the deviations increase at higher pressures. The deviations become increasingly negative down to −3.2% at 100 MPa. The speed of sound data at ambient pressure between 290 K and 373 K are represented by the equation within 0.2%.

For the **isobaric heat capacity**, there are fewer experimental data than those of the properties previously discussed. The measurements, shown in Figure 8, are within 6% from the equation. The work with the largest number of measurements is that of Banipal *et al.* [10]. They are well represented by the equation of state; the deviations are not higher than 0.3% in the temperature range from 318 K and 373 K. At 298 K, the measurements of Benson *et al.* [12] deviate from the equation by less than 0.02%. The deviations of their data increase to 0.5% for higher temperatures (up to 358 K), and all of them are negative.

**Comparison to *n*-docosane experimental data**

For *n*-docosane, there are significantly fewer data points than for *n*-hexadecane. The **vapor pressure** is the most studied property for this fluid, covering a wide range of temperature (see Figure 9). The data set of Morgan and Kobayashi [49] is best represented by the equation at high temperatures, between 453 K and 573 K, with an average deviation of 0.5%. The data given in Sasse *et al.* [67] show different behavior depending on the temperature. Between 393 K and 423 K, the data spread about the equation within 2%. Below 393 K, they all show deviations between −4% and −8%. Above 423 K the data differ with the equation consistently around 2%. The data of Chickos and Hanshaw [19] show deviations consistently around −2% at temperatures higher than 450 K, while the data and equation differ more as the temperature decreases.

All the experimental **saturated liquid densities** deviate from the equation of state within ±0.2%, as shown in Figure 10. The measurements of Dutour *et al.* [23] deviate more from the equation as the temperature increases, starting from −0.001% at 323.15 K to −0.12% at 393.15 K. Queimada *et al.* [66] measured three saturated liquid density points, which deviate from the calculated values by around −0.06%. The measurements of Neruchev *et al.* [53] cover a wider range of temperature, from 333 K to 473 K; all of them agree with the equation of state within ±0.15%.

Peters *et al.* [57] published the only ***pvT*** data reported for *n*-docosane, with temperatures from 323 K to 368 K and pressures up to 16 MPa. As shown in Figure 11, the data show a systematic average deviation of −1% from the equation of state. The data at pressures near ambient differ from the saturated liquid density data by this amount. The data show a consistent offset from the equation at all pressures.

The measurements of Neruchev *et al.* [53] and Dutour *et al.* [23] are the only available data for *n*-docosane for the **speed of sound** as shown in Figure 12. Between 353 K and 373 K the two sets overlap, and the deviations from the equation and both sets are lower than 0.2% at ambient pressure. Over their whole temperature range (from 333 K to 473 K) the Neruchev data are accurately represented by the equation of state, with a maximum deviation of 0.2%. The data presented by Dutour *et al.* deviate from the equation of state within 1%, but for the measurements performed at ambient pressure, the maximum deviation is less than 0.3%.

For the **isobaric heat capacity**, just two sets of data are available: Atkinson *et al.* [6] and Durupt *et al.* [22]. The two data sets show substantial differences at the higher temperatures as shown in Figure 13. The deviations of the Atkinson *et al.* data are within 0.05% and −0.5%, while the deviations of the Durupt *et al.* data increase with increasing temperatures, from 2.2% at 273 K and up to 8% at 473 K.

VIRIAL COEFFICIENTS

One of the most important validation tests in the development of equations of state comes from the analysis of its virial coefficients.

$$Z(T,\rho) = 1 + B(T)\rho + C(T)\rho^2 + D(T)\rho^3 + \ \ldots \tag{15}$$

In Figure 2, a plot of the second, third, and fourth virial coefficients is given as a function of temperature. The third virial coefficient *C* for *n*-hexadecane has a maximum value of 1.849 $dm^6/mol^2$ at 486.3 K, and is always positive above a temperature of 367.14 K. The maximum value of the fourth virial

coefficient $D$ is 1.120 $dm^9/mol^3$ at 489.3 K, has a minimum positive value at 1304 K and a second maximum around 7536 K (for any temperature between 1304 K and above). These values and the shape of the function were achieved through the use of the constraints reported in Table 5 and explained in the section "Fitting constraints".

## EXTRAPOLATION BEHAVIOUR

The REFPROP software [92] was used to generate diagrams for inspection of the extrapolation behavior. One of the most important parameters used to verify the correct behavior of the equations is the phase identification parameter (PIP) defined in the work of Venkatarathnam and Oellrich [90]; this is an extremely sensitive property from which small inconsistencies can be seen that are not visible with other properties.

In Figure 14 the PIP for *n*-hexadecane as a function of temperature is shown, along isobars and at saturation states. The plot shows positive curvature in the PIP over most of the liquid region, except for the region between 150 K and about 200 K. At very low temperatures (below 20 K), the curvature is still negative. This behavior of the PIP is also present in the plots for R-1234ze(E) reported in the work of Thol and Lemmon [93] and for R-245ca reported in Zhou and Lemmon [94].

Similar behavior is observed in the plot of the PIP versus temperature for *n*-docosane, shown in Figure 15. The curvature is almost always positive over the liquid region, although it becomes slightly negative between 175 K and 205 K. The PIP for *n*-docosane, even at temperatures lower than 15 K, has positive curvature.

The validation of the equations can also be done by checking the behavior of other properties such as density, speed of sound, heat capacity, and the ideal curves. All of these properties show the expected trends as explained in other publications on equations of state, such as the work for the equation of state of propane [88] or R-125 [95].

The ideal curves are curves along which one property of a real fluid is equal to the hypothetical ideal gas. This definition can refer to any property, but usually the ideal curves of the compressibility factor, $Z(T, \rho)$, and its derivatives are only considered, as follows

Ideal curve:

$$Z = 1$$

Boyle curve:

$$\left(\frac{\partial Z}{\partial \rho}\right)_T = 0$$

Joule-Thomson curve:

$$\left(\frac{\partial Z}{\partial T}\right)_p = 0$$

Joule inversion curve:

$$\left(\frac{\partial Z}{\partial T}\right)_\rho = 0$$

The ideal curves are used to judge the behavior of the equation of state. Even if the curves do not provide numerical information, reasonable shapes of the curves, such as the plots for propane [88], indicate correct extrapolation behavior of the equation of state extending to high pressures and temperatures far in excess of the likely thermal stability of the fluid. Consequently, the behavior of the ideal curves should always be analyzed and checked during the equation development process. Figures 16 and 17 show the plots of the ideal curves obtained for *n*-hexadecane and *n*-docosane, which have the expected shape, giving confidence in the proper extrapolation behavior at high temperatures and pressures.

## CONCLUSIONS

Fundamental equations of state for *n*-hexadecane and *n*-docosane were developed and presented here. The equations can be used to calculate all the thermodynamic properties of these alkanes over the entire fluid region.

For *n*-hexadecane, the uncertainty in vapor pressure is 0.5%. For saturated liquid density, the uncertainty is 0.05% for temperatures up to 400 K and increases to 0.2% at higher temperatures. The estimated uncertainty in densities is 0.1% from the triple point to 450 K for pressures below 50 MPa. Outside this range, the uncertainty is 0.5%. The speed of sound has an uncertainty of 0.25%. The uncertainty in isobaric heat capacity is estimated to be 0.25%.

For *n*-docosane, the uncertainty in vapor pressure is about 5% and the uncertainty in saturated liquid density is 0.1%. At pressures up to 20 MPa, the uncertainty in density is about 1%; no estimation can be provided at higher pressures. For speed of sound, the uncertainty is less than 0.5% at ambient pressure and increases to 1% at higher pressures. The uncertainty in heat capacity is 3%.

## SUPPLEMENTARY INFORMATION

The files containing the parameters of the equations of state for *n*-hexadecane and *n*-docosane are available for the use in REFPROP [92], TREND [96], and CoolProp [97].

## DECLARATIONS

**Conflict of interest** The authors have no competing interests to declare that are relevant to the content of this article.

Table 6. Experimental data for *n*-hexadecane.

| Authors | | # Pnts. | Temperature Range (K) | Pressure Range (MPa) | Density Range (mol/l) | AAD (%) |
|---|---|---|---|---|---|---|
| | | | Vapor pressure | | | |
| Abedinzadegan Abdi and Meisen (1998) | [1] | 8 | 393-482 | 0-0.013 | | 7.36 |
| Camin *et al.* (1954) | [17] | 16 | 463-560 | 0.007-0.101 | | 0.066 |
| Eggertsen *et al.* (1969) | [28] | 10 | 299-413 | 0 | | 3.38 |
| Francis and Wood (1926) | [33] | 4 | 410-435 | 0.001-0.003 | | 6.61 |
| Grenier-Loustalot *et al.* (1981) | [38] | 4 | 358-418 | 0-0.001 | | 4.85 |
| Krafft (1882) | [40] | 6 | 424-561 | 0.001-0.101 | | 2.75 |
| Lee *et al.* (1992) | [43] | 5 | 504-589 | 0.026-0.188 | | 1.76 |
| Mills and Fenton (1987) | [46] | 11 | 389-560 | 0-0.102 | | 0.841 |
| Morgan and Kobayashi (1994) | [49] | 20 | 393-583 | 0-0.164 | | 0.223 |
| Myers and Fenske (1955) | [50] | 26 | 354-559 | 0-0.101 | | 3.25 |
| Parks and Moore (1949) | [56] | 10 | 298-323 | 0 | | 10.1 |
| Siitsman *et al.* (2014) | [69] | 5 | 486-561 | 0.015-0.102 | | 0.863 |
| Viton *et al.* (1996) | [74] | 24 | 303-467 | 0-0.008 | | 2.92 |
| Zuiderweg (1952) | [83] | 31 | 371-464 | 0-0.007 | | 5.8 |
| TDE | [84] | 43 | 282-561 | 0-0.102 | | 20 |
| | | | Saturated liquid density | | | |
| Aminabhavi *et al.* (1992) | [2] | 6 | 298-323 | | 3.33-3.41 | 0.117 |
| Asfour *et al.* (1990) | [5] | 4 | 293-313 | | 3.36-3.42 | 0.057 |
| Banos *et al.* (1992) | [11] | 7 | 293-323 | | 3.32-3.42 | 0.023 |
| Boelhouwer (1960) | [13] | 4 | 303-393 | | 3.11-3.39 | 0.018 |
| Bolotnikov *et al.* (2005) | [15] | 17 | 293-373 | | 3.17-3.42 | 0.025 |
| Calingaert *et al.* (1941) | [16] | 4 | 293-373 | | 3.17-3.42 | 0.043 |
| Diaz Pena and Tardajos (1978) | [20] | 4 | 298-333 | | 3.29-3.4 | 0.016 |
| Doolittle (1964) | [21] | 6 | 323-573 | | 2.49-3.35 | 0.524 |
| Dymond *et al.* (1979) | [26] | 4 | 298-373 | | 3.17-3.4 | 0.065 |
| Dymond and Young (1980) | [25] | 11 | 298-393 | | 3.11-3.4 | 0.075 |
| Dymond *et al.* (1980) | [27] | 7 | 298-358 | | 3.22-3.4 | 0.056 |
| El-Banna and El-Batouti (1998) | [29] | 7 | 283-313 | | 3.36-3.43 | 0.055 |
| Espeau and Ceolin (2006) | [30] | 12 | 298-573 | | 2.44-3.36 | 1.61 |
| Findenegg (1970) | [31] | 7 | 293-333 | | 3.29-3.42 | 0.015 |
| Graaf *et al.* (1992) | [37] | 5 | 375-538 | | 2.65-3.17 | 0.311 |
| Krafft (1882) | [40] | 4 | 291-372 | | 3.18-3.42 | 0.104 |
| Lauer and King (1956) | [42] | 7 | 298-368 | | 3.19-3.4 | 0.04 |
| Paredes *et al.* (2011) | [55] | 6 | 293-343 | | 3.26-3.42 | 0.03 |
| Plebanski *et al.* (1986) | [62] | 11 | 300-490 | | 2.79-3.39 | 0.067 |
| Prak *et al.* (2013) | [63] | 9 | 293-373 | | 3.17-3.42 | 0.017 |
| Prak *et al.* (2014) | [64] | 9 | 293-373 | | 3.17-3.42 | 0.026 |
| Queimada *et al.* (2003) | [65] | 6 | 293-343 | | 3.26-3.42 | 0.021 |
| Schiessler *et al.* (1946) | [68] | 5 | 273-372 | | 3.18-3.48 | 0.03 |
| Vogel (1946) | [75] | 4 | 293-360 | | 3.22-3.42 | 0.174 |
| Wu *et al.* (1998) | [77] | 4 | 293-313 | | 3.35-3.41 | 0.065 |
| TDE | [84] | 117 | 281-414 | | 3.05-4.02 | 0.115 |
| | | | Density | | | |
| Amorim *et al.* (2007) | [4] | 54 | 318-413 | 6.89-62.1 | 3.07-3.5 | 0.126 |
| Banipal *et al.* (1991) | [10] | 72 | 318-373 | 0.1-10 | 3.17-3.37 | 0.023 |
| Boelhouwer (1960) | [13] | 44 | 303-393 | 0.101-118 | 3.11-3.56 | 0.156 |
| Chang *et al.* (1998) | [18] | 21 | 333-413 | 0.1-30 | 3.05-3.39 | 0.132 |
| Doolittle (1964) | [21] | 60 | 323-573 | 5-500 | 2.57-4 | 0.756 |

| | | | | | | |
|---|---|---|---|---|---|---|
| Dymond *et al.* (1979) | [26] | 27 | 298-373 | 0.1-450 | 3.17-3.9 | 0.061 |
| Dymond and Harris (1992) | [24] | 23 | 298-348 | 0.1-279 | 3.25-3.77 | 0.06 |
| Glaser *et al.* (1985) | [34] | 63 | 303-360 | 2.03-17.7 | 3.21-3.44 | 0.221 |
| Gouel (1978) | [36] | 75 | 315-392 | 5.17-40.6 | 3.13-3.47 | 0.068 |
| Matthews *et al.* (1987) | [44] | 10 | 323-564 | 1.42-3.5 | 2.54-3.33 | 0.313 |
| Outcalt *et al.* (2010) | [54] | 108 | 291-470 | 0.083-50.7 | 2.86-3.46 | 0.108 |
| Snyder and Winnick (1970) | [70] | 93 | 298-358 | 0.101-290 | 3.22-3.75 | 0.095 |
| Tanaka *et al.* (1991) | [71] | 16 | 298-348 | 0.1-150 | 3.25-3.64 | 0.065 |
| Wu *et al.* (2011) | [78] | 31 | 324-523 | 14.1-262 | 2.84-3.63 | 0.15 |
| Wuerflinger *et al.* (2001) | [79] | 27 | 298-313 | 0.1-90 | 3.36-3.58 | 0.078 |
| Wuerflinger and Sandmann (2000) | [80] | 104 | 303-348 | 0.1-280 | 3.27-3.79 | 0.683 |
| Zolghadr *et al.* (2013) | [82] | 165 | 313-393 | 0.34-11.4 | 3.14-3.39 | 0.352 |
| | | | Enthalpy of vaporization | | | |
| Morawetz (1968) | [47] | 4 | 298 | | | 2.1 |
| Morawetz (1972) | [48] | 1 | 298 | | | 0.762 |
| | | | Heat capacity | | | |
| Baba *et al.* (1992) | [8] | 11 | 323-423 | 5 | | 3.71 |
| Banipal *et al.* (1991) | [10] | 60 | 318-373 | 0.1-10 | | 0.124 |
| Benson *et al.* (1971) | [12] | 4 | 298-358 | 0.101 | | 0.315 |
| Gollis *et al.* (1962) | [35] | 3 | 311-422 | 0.101 | | 3.64 |
| Lainez *et al.* (1989) | [41] | 1 | 298 | | | 0.739 |
| Petit and Ter Minassian (1974) | [58] | 14 | 298-454 | 0.101 | | 1.16 |
| Tardajos *et al.* (1986) | [72] | 1 | 298 | | | 0.243 |
| Wilhelm *et al.* (1986) | [76] | 1 | 298 | | | 1.03 |
| | | | Saturation heat capacity | | | |
| Finke *et al.* (1954) | [32] | 84 | 11.9-320 | | | 0.101 |
| | | | Speed of sound | | | |
| Aminabhavi and Gopalakrishna (1994) | [3] | 3 | 298-318 | | | 0.693 |
| Awwad and Pethrick (1984) | [7] | 1 | 298 | 0.101 | | 0.144 |
| Ball and Trusler (2001) | [9] | 65 | 298-373 | 0.1-101 | | 0.416 |
| Boelhouwer (1967) | [14] | 74 | 293-473 | 10-140 | | 0.259 |
| Bolotnikov *et al.* (2005) | [15] | 17 | 293-373 | 0.1 | | 0.125 |
| Khasanshin and Shchemelev (2001) | [39] | 29 | 303-433 | 0.1-49.1 | | 0.106 |
| Nascimento *et al.* (2015) | [51] | 18 | 313-333 | 0.1-25 | | 0.116 |
| Neruchev *et al.* (2005) | [52] | 43 | 293-713 | 0.1 | | 3.21 |
| Outcalt *et al.* (2010) | [54] | 16 | 291-343 | 0.083 | | 0.029 |
| Paredes *et al.* (2011) | [55] | 6 | 293-343 | 0.101 | | 0.034 |
| Plantier *et al.* (2000) | [61] | 9 | 303-383 | | | 0.638 |
| Prak *et al.* (2014) | [64] | 5 | 293-333 | 0.1 | | 0.025 |
| Tardajos *et al.* (1986) | [73] | 1 | 298 | | | 0.407 |

Table 7. Experimental data for *n*-docosane.

| Authors | | # Pnts. | Temperature Range (K) | Pressure Range (MPa) | Density Range (mol/l) | AAD (%) |
|---|---|---|---|---|---|---|
| | | | Vapor pressure | | | |
| Chickos and Hanshaw (2004) | [19] | 11 | 298-575 | 0-0.021 | | 7.18 |
| Francis and Wood (1926) | [33] | 8 | 462-509 | 0-0.004 | | 21.3 |
| Grenier-Loustalot *et al.* (1981) | [38] | 4 | 379-434 | 0 | | 3.16 |
| Morgan and Kobayashi (1994) | [49] | 12 | 453-573 | 0-0.021 | | 0.459 |
| Piacente *et al.* (1991) | [60] | 115 | 341-489 | 0 | | 28.4 |
| Piacente *et al.* (1994) | [59] | 23 | 372-410 | 0 | | 26.4 |

| | | | | | | |
|---|---|---|---|---|---|---|
| Sasse *et al.* (1988) | [67] | 16 | 353-462 | 0 | | 3 |
| Young (1928) | [81] | 3 | 494-519 | 0.001-0.004 | | 5.44 |
| | | | Saturated liquid density | | | |
| Melaugh *et al.* (1976) | [45] | 1 | 323 | | 2.5 | 0.088 |
| Queimada *et al.* (2005) | [66] | 3 | 323-343 | | 2.45-2.49 | 0.057 |
| Dutour *et al.* (2001) | [23] | 8 | 323-393 | | 2.34-2.49 | 0.053 |
| Neruchev *et al.* (1967) | [53] | 15 | 333-473 | | 2.17-2.48 | 0.059 |
| | | | Density | | | |
| Peters *et al.* (1988) | [57] | 48 | 323-368 | 2.05-16.1 | 2.38-2.51 | 0.945 |
| | | | Heat capacity | | | |
| Durupt *et al.* (1996) | [22] | 6 | 373-473 | 0.101 | | 5.23 |
| Atkinson *et al.* (1969) | [6] | 8 | 320-450 | 0.101 | | 0.255 |
| | | | Speed of sound | | | |
| Dutour *et al.* (2001) | [23] | 126 | 323-393 | 0.101-150 | | 0.559 |
| Neruchev *et al.* (1967) | [53] | 15 | 333-473 | 0.1 | | 0.064 |

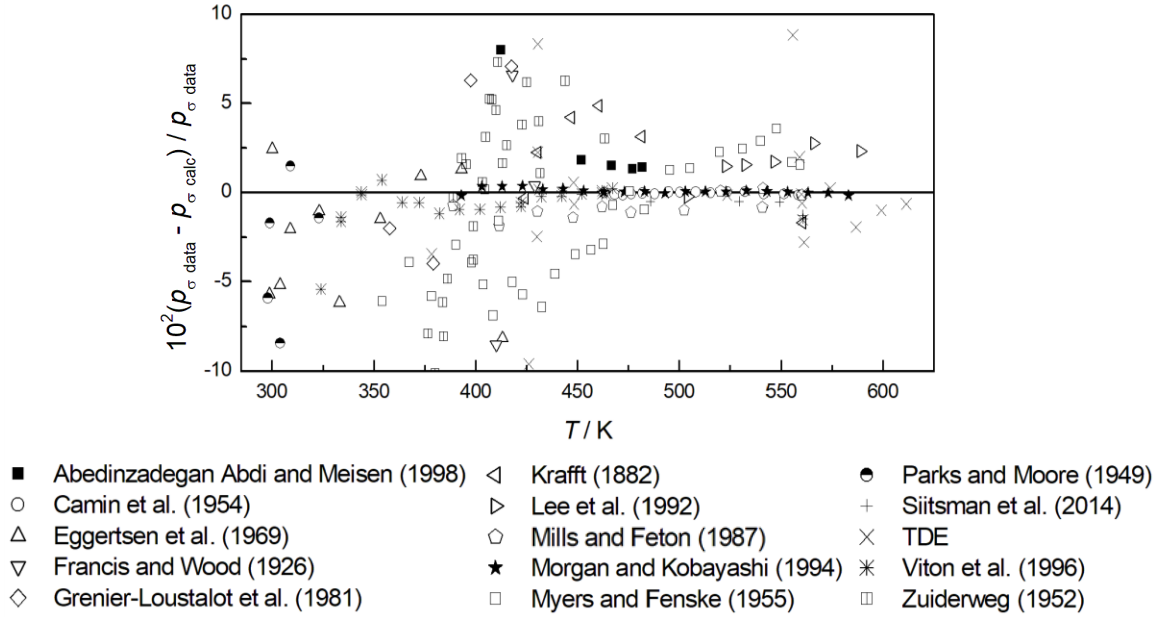


Figure 4. Comparisons of $C_{16}H_{34}$ vapor pressures $p_\sigma$ calculated with the equation of state and experimental data.

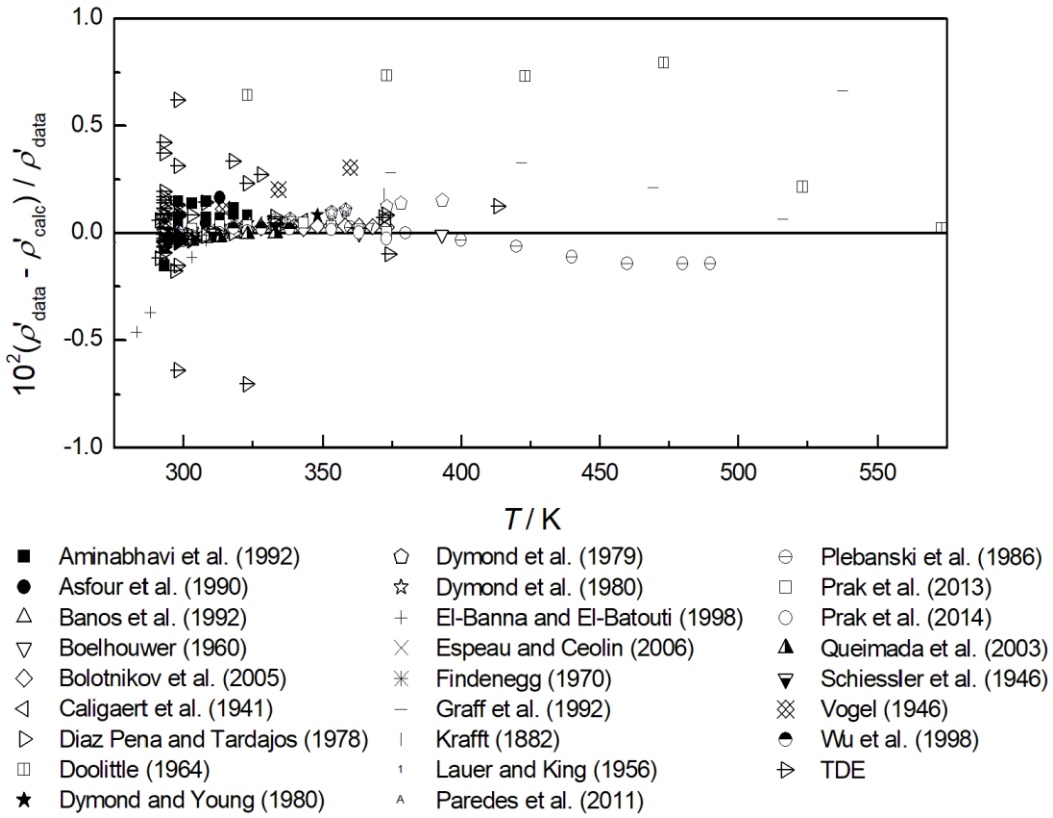


Figure 5. Comparisons of $C_{16}H_{34}$ saturated liquid densities $\rho'$ calculated with the equation of state and experimental data.

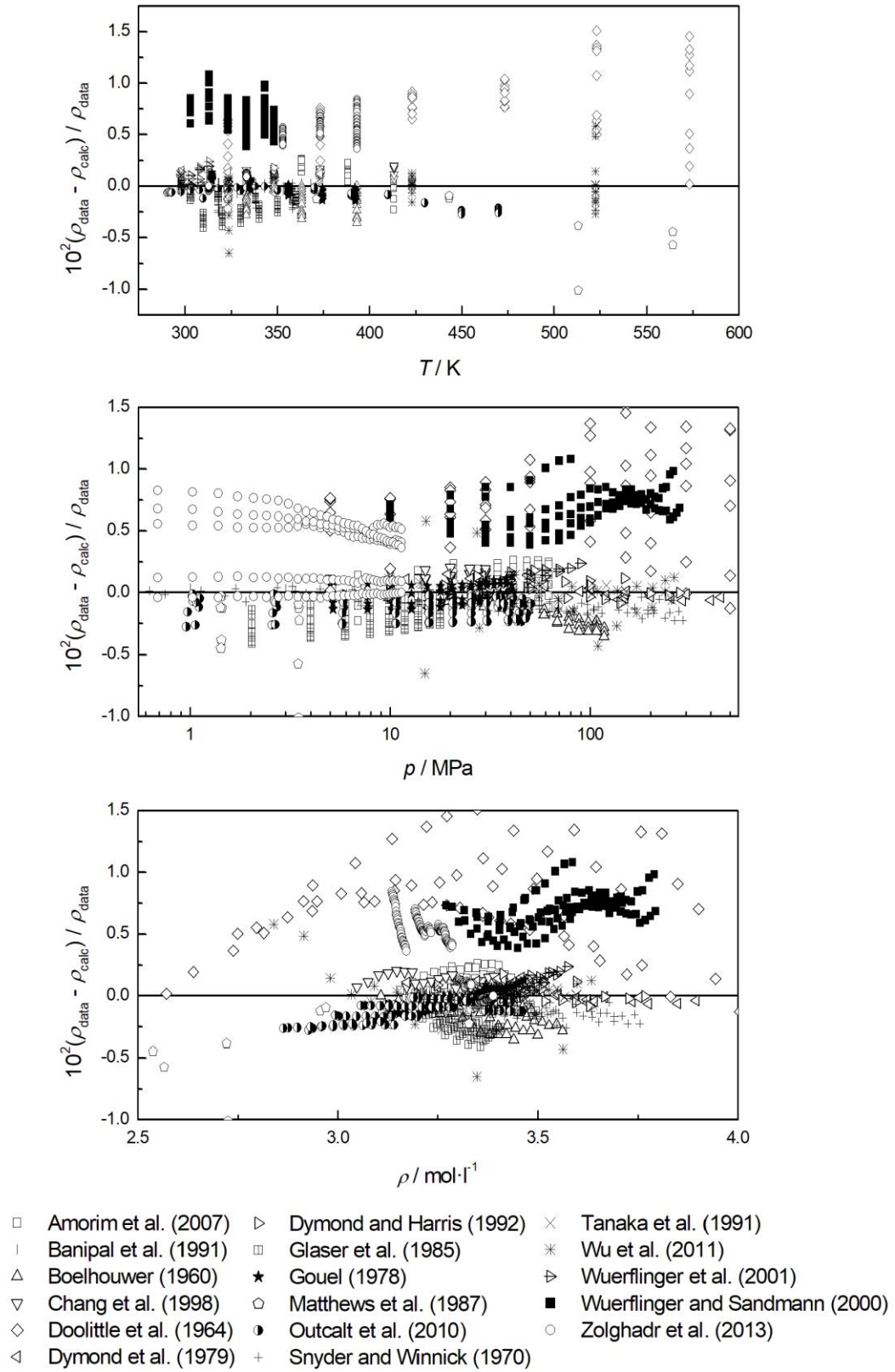


Figure 6. Comparisons of $C_{16}H_{34}$ densities $\rho$ calculated with the equation of state and experimental data.

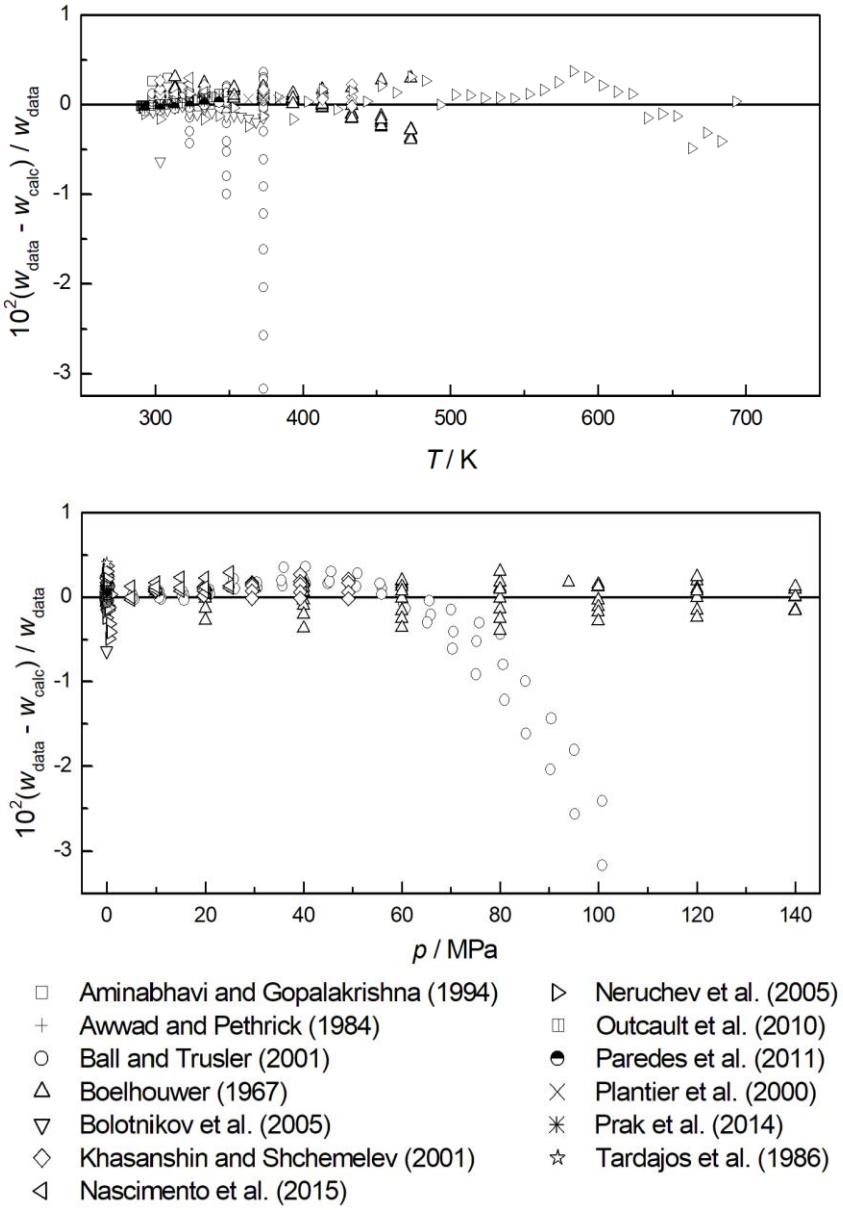


Figure 7. Comparisons of $C_{16}H_{34}$ speeds of sound $w$ calculated with the equation of state and experimental data.

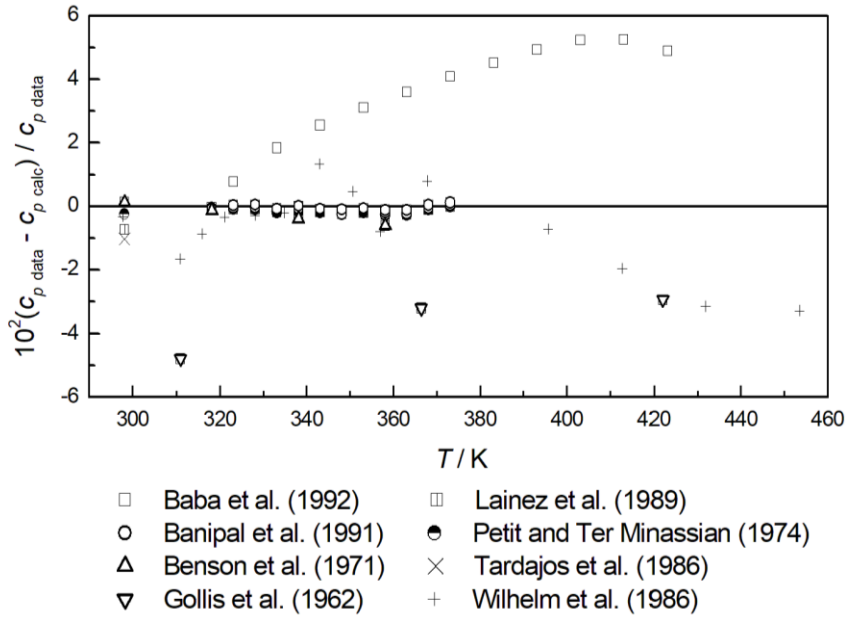


Figure 8. Comparisons of $C_{16}H_{34}$ heat capacities $c_p$ calculated with the equation of state and experimental data.

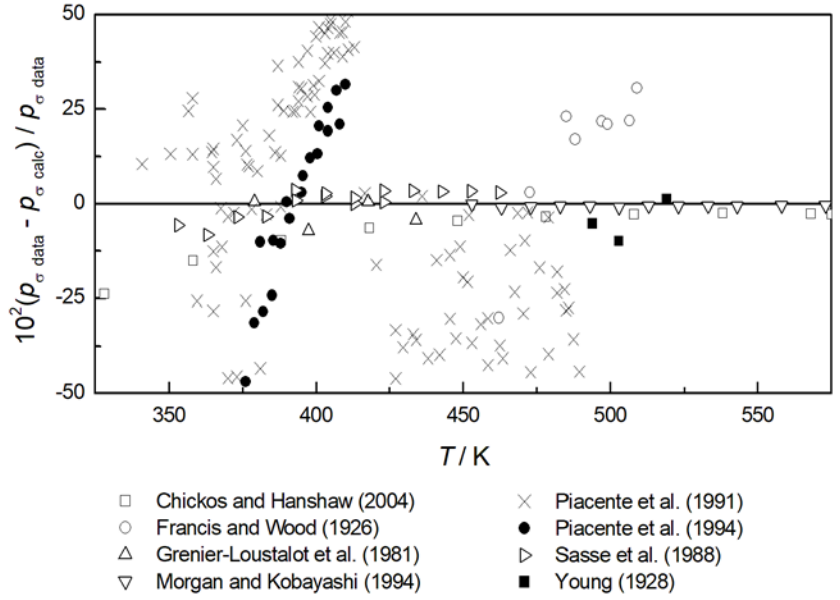


Figure 9. Comparisons of $C_{22}H_{46}$ vapor pressures $p_\sigma$ calculated with the equation of state and experimental data.

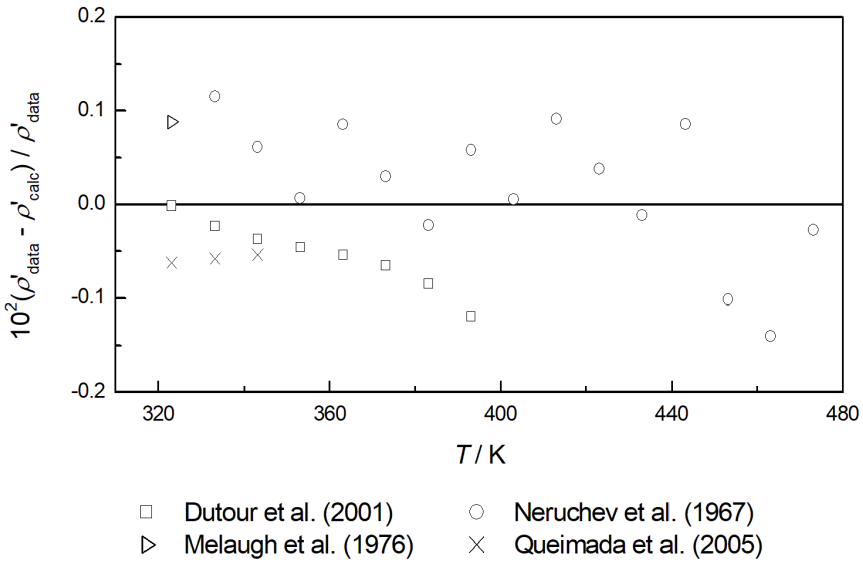


Figure 10. Comparisons of $C_{22}H_{46}$ saturated liquid densities $\rho'$ calculated with the equation of state and experimental data.

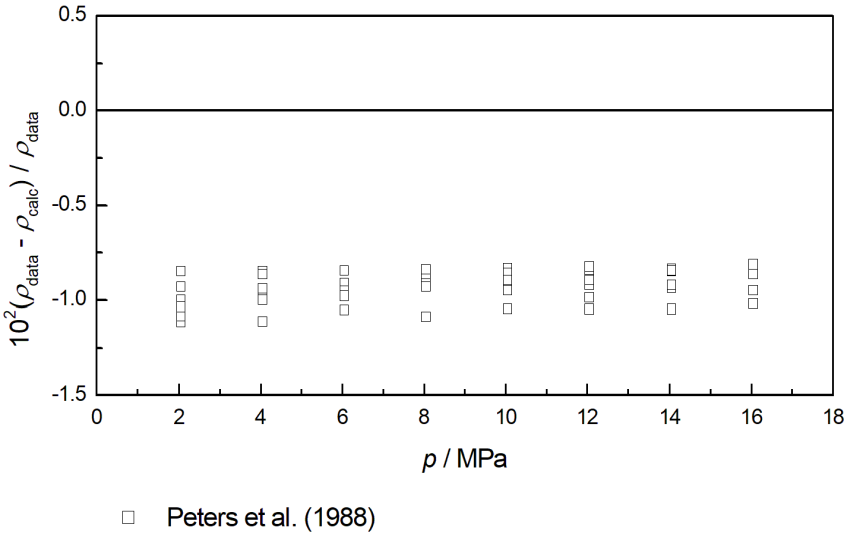


Figure 11. Comparisons of $C_{22}H_{46}$ densities $\rho$ calculated with the equation of state and experimental data.

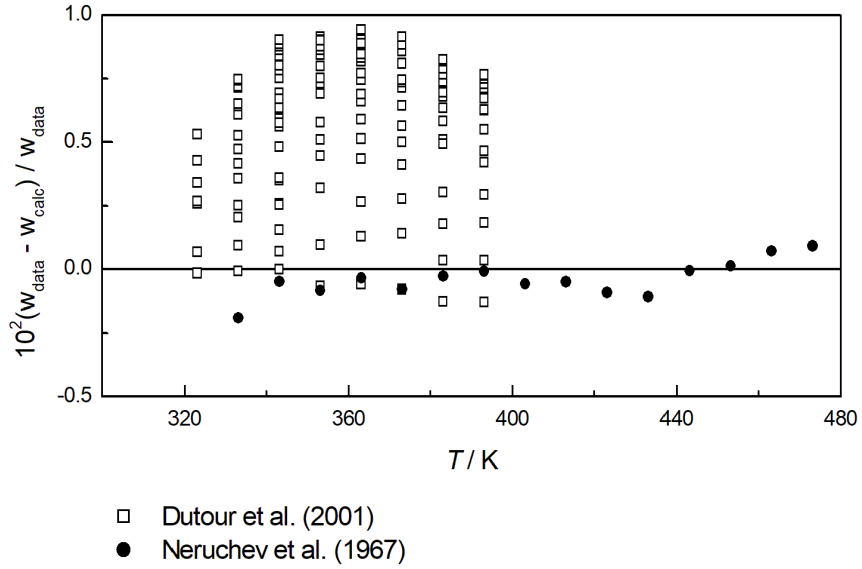


Figure 12. Comparisons of $C_{22}H_{46}$ speeds of sound $w$ calculated with the equation of state and experimental data.

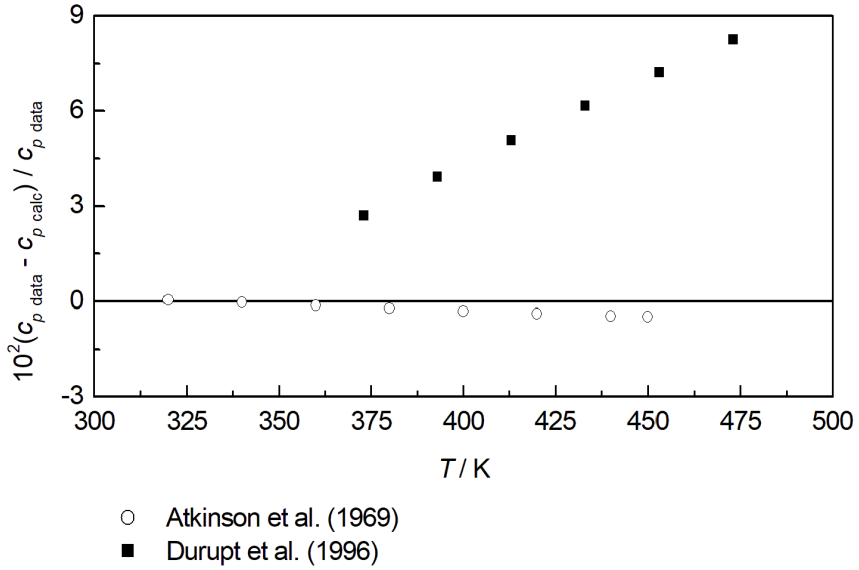


Figure 13. Comparisons of $C_{22}H_{46}$ heat capacities $c_p$ calculated with the equation of state and experimental data.

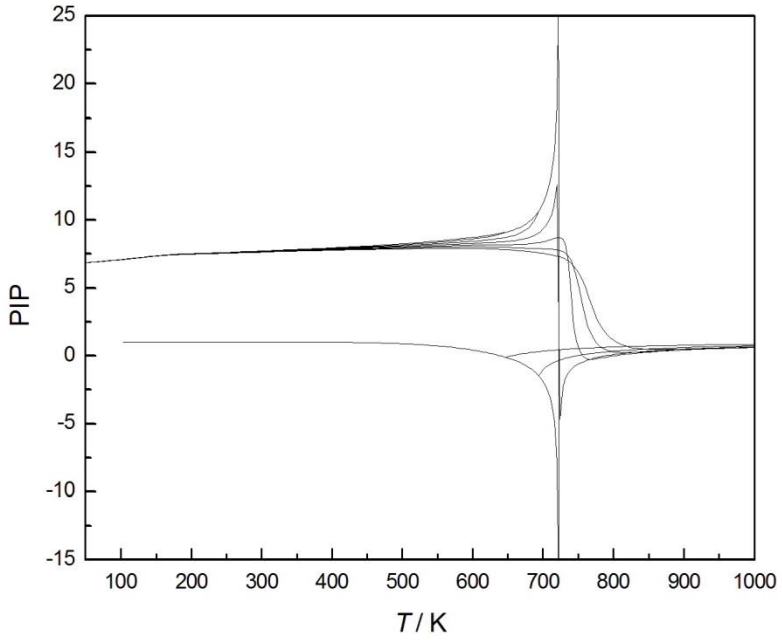


Figure 14. Phase identification parameter (PIP) as a function of temperature for *n*-hexadecane along isobars from 0.5 MPa to 3 MPa.

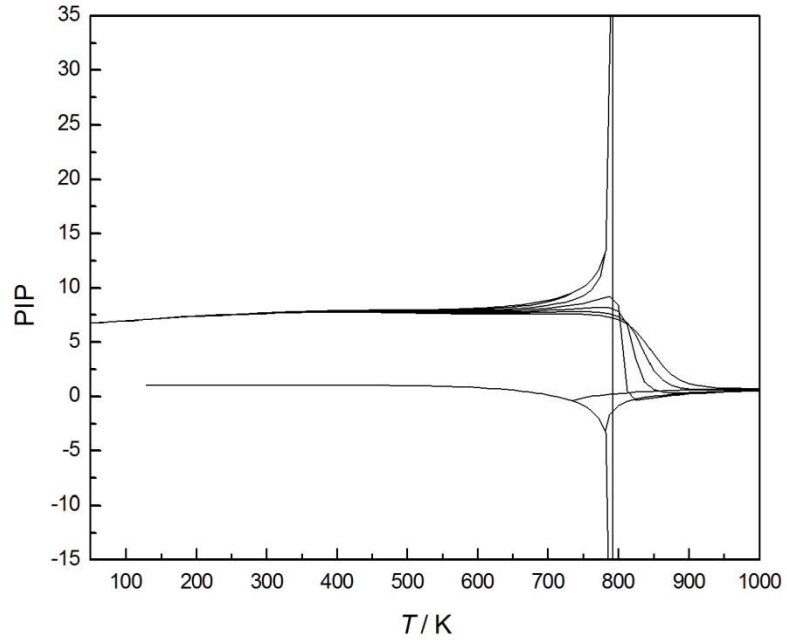


Figure 15. Phase identification parameter (PIP) as a function of temperature for *n*-docosane along isobars from 0.5 MPa to 3 MPa.

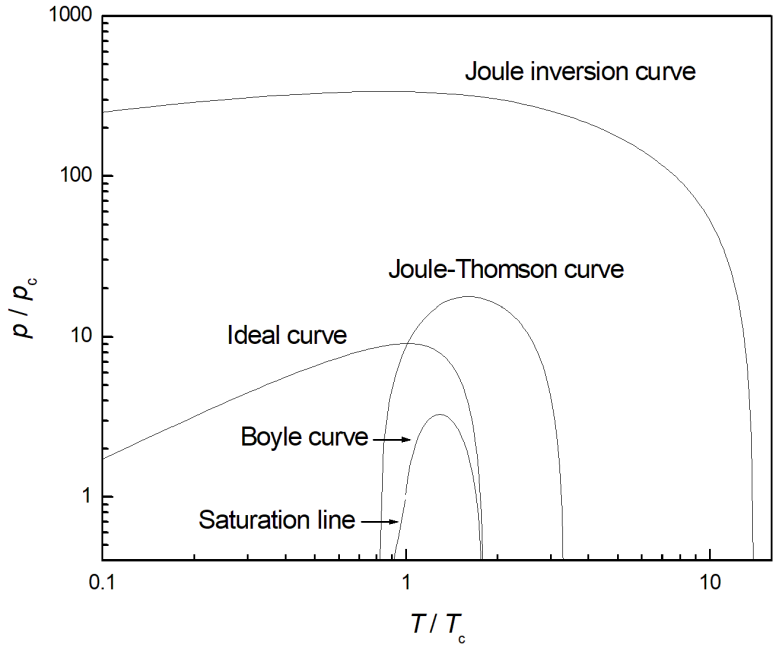


Figure 16. Ideal curves for *n*-hexadecane.

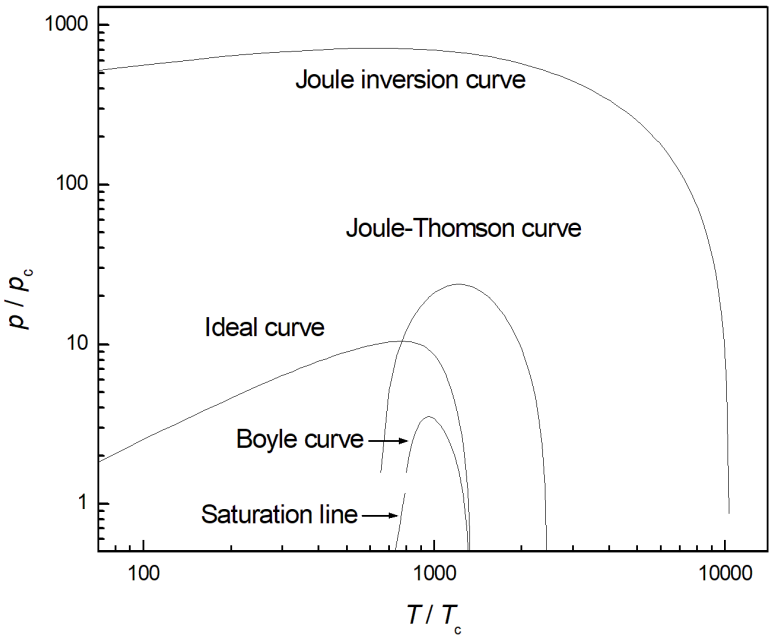


Figure 17. Ideal curves for *n*-docosane.

REFERENCES


1. Abedinzadegan Abdi, M.; Meisen, A. Vapor Pressure Measurements of Bis(hydroxyethyl)piperazine and Tris(hydroxyethyl)ethylenediamine. J. Chem. Eng. Data 1998, 43, 133-137.
2. Aminabhavi, T. M.; Aralaguppi, M. I.; Harogoppad, S. B.; Balundgi, R. H. Polarizability and Molecular Radius of Bromoform and Hydrocarbon Liquids. Fluid Phase Equilib. 1992, 72, 211-225.
3. Aminabhavi, T. M.; Gopalakrishna, B. Densities, Viscosities, Refractive Indices, and Speeds of Sound of the Binary Mixtures of Bis(2-Methoxyethyl) Ether with Nonane, Decane, Dodecane, Tetradecane, and Hexadecane at 298.15, 308.15, and 318.15 K. J. Chem. Eng. Data 1994, 39, 529-534.
4. Amorim, J. A.; Chiavone-Filho, O.; Paredes, M. L. L.; Rajagopal, K. High-Pressure Density Measurements for Binary System Cyclohexane + *n*-Hexadecane in the Temperature Range of (318.15 to 413.15) K. J. Chem. Eng. Data 2007, 52, 613-618.
5. Asfour, A.-F. A.; Siddique, M. H.; Vavanellos, T. D. Density-Composition Data for Eight Binary Systems Containing Toluene or Ethylbenzene and $C_8$-$C_{16}$ *n*-Alkanes at 293.15, 298.15, 308.15, and 313.15 K. J. Chem. Eng. Data 1990, 35, 192-198.
6. Atkinson, C. M. L.; Larkin, J. A.; Richardson, M. J. Enthalpy Changes in Molten *n*-Alkanes and Polyethylene. J. Chem. Thermodyn. 1969, 1, 435-440.
7. Awwad, A. M.; Pethrick, R. A. Isentropic Compressibilities of Hydrocarbons and their Mixtures. Mixtures of Linear and Branched-Chain Alkanes. J. Chem. Thermodyn. 1984, 16, 131-136.
8. Baba, M.; Dordain, L.; Coxam, J.-Y.; Grolier, J.-P. E. Calorimetric Measurements of Heat Capacities and Heats of Mixing in the Range 300-570 K and up to 30 MPa. Indian J. Tech. 1992, 30, 553-558.
9. Ball, S. J.; Trusler, J. P. M. Speed of Sound of *n*-Hexane and *n*-Hexadecane at Temperatures between 298 and 373 K and Pressures up to 100 MPa. Int. J. Thermophys. 2001, 22, 427-443.

10. Banipal, T. S.; Garg, S. K.; Ahluwalia, J. C. Heat Capacities and Densities of Liquid *n*-Octane, *n*-Nonane, *n*-Decane, and *n*-Hexadecane at Temperatures from 318.15 K to 373.15 K and at Pressures up to 10 MPa. J. Chem. Thermodyn. 1991, 23, 923-931.
11. Banos, I.; Sanchez, F.; Perez, P.; Valero, J.; Gracia, M. Vapor Pressures of Butan-1-ol with *n*-Hexadecane between 293.18 and 323.18 K. Description of Butan-1-ol + *n*-Alkane Systems by ERAS Model. Fluid Phase Equilib. 1992, 81, 165-174.
12. Benson, M. S.; Snyder, P. S.; Winnick, J. Heat Capacities of Liquid *n*-Alkanes at Elevated Pressures. J. Chem. Thermodyn. 1971, 3, 891-898.
13. Boelhouwer, J. W. M. PVT Relations of Five Liquid *n*-Alkanes. Physica 1960, 26, 1021-1028.
14. Boelhouwer, J. W. M. Sound Velocities in and Adiabatic Compressibilities of Liquid Alkanes at Various Temperatures and Pressures. Physica 1967, 34, 484-492.
15. Bolotnikov, M. F.; Neruchev, Y. A.; Melikhov, Y. F.; Verveyko, V. N; Verveyko, M. V. Temperature Dependence of the Speed of Sound, Densities, and Isoentropic Compressibilities of Hexane + Hexadecane in the Range of (293.15 to 373.15) K. J. Chem. Eng. Data 2005, 50, 1095-1098.
16. Calingaert, G.; Beatty, H. A.; Kuder, R. C.; Thomson, G. W. Homologous Series of Alkanes Density and its Temperature Coefficient. Ind. Eng. Chem. 1941, 33, 103-106.
17. Camin, D. L.; Forziati, A. F.; Rossini, F. D. Physical Properties of *n*-Hexadecane, *n*-Deccylcyclopentane, *n*-Deccylcyclohexane, 1-Hexadecene and *n*-Decylbenzene. J. Phys. Chem. 1954, 58, 440-442.
18. Chang, J.; Lee, M.; Lin, H. Densities of Binary Mixtures of Hexadecane with *m*-Xylene and Tetralin from 333 K to 413 K and Pressures up to 30 MPa. J. Chem. Eng. Data 1998, 43, 233-237.
19. Chickos, J. S.; Hanshaw, W. Vapor Pressures and Vaporization Enthalpies of the *n*-Alkanes from $C_{21}$ to $C_{30}$ at $T$=298.15 K by Correlation Gas Chromatography. J. Chem. Eng. Data 2004, 49, 77-85.
20. Diaz Pena, M.; Tardajos, G. Isothermal Compressibilities of *n*-Alkanes and Benzene. J. Chem. Thermodyn. 1978, 10, 19-24.
21. Doolittle, A. K. Specific Volumes of *n*-Alkanes. J. Chem. Eng. Data 1964, 9, 275-279.
22. Durupt, N.; Aoulmi, A.; Bouroukba, M.; Rogalski, M. Heat Capacities of Liquid Long-Chain Alkanes. Thermochim. Acta 1996, 274, 73-80.
23. Dutour, S.; Daridon, J. L., Lagourette, B. Speed of Sound, Density, and Compressibilities of Liquid Eicosane and Docosane at Various Temperatures and Pressures. High Temp.-High Press. 2001, 33, 371-378.
24. Dymond, J. H.; Harris, K. R. The Temperature and Density Dependence of the Self-Diffusion Coefficient of n-Hexadecane. Mol. Phys. 1992, 75, 461-466.
25. Dymond, J. H.; Young, K. J. Transport Properties of Nonelectrolyte Liquid Mixtures - I. Viscosity Coefficients for *n*-Alkane Mixtures at Saturation Pressure from 283 to 378 K. Int. J. Thermophys. 1980, 1, 331-344.
26. Dymond, J. H.; Young, K. J.; Isdale, J. D. $p$, $\rho$, $T$ Behaviour for *n*-Hexane + *n*-Hexadecane in the Range 298 to 373 K and 0.1 to 500 MPa. J. Chem. Thermodyn. 1979, 11, 887-895.
27. Dymond, J. H.; Young, K. J.; Isdale, J. D. Transport Properties of Nonelectrolyte Liquid Mixtures - II. Viscosity Coefficients for the *n*-Hexane + *n*-Hexadecane System at Temperatures from 25 to 100 °C at Pressures up to the Freezing Pressure or 500 MPa. Int. J. Thermophys. 1980, 1, 345-373.
28. Eggertsen, F. T.; Seibert, E. E.; Stross, F. H. Volatility of High Boiling Organic Materials by a Flame Ionization Detection Method. Anal. Chem. 1969, 41, 1175-1179.
29. El-Banna, M. M.; El-Batouti, M. M. Temperature Dependence of the Excess Volumes of Binary Mixtures Containing Cyclohexane + Some Higher *n*-Alkanes. Can. J. Chem. 1998, 76, 1860-1866.

30. Espeau, P.; Ceolin, R. A Simple Method to Determine the Specific Volumes of Liquids and Melts as a Function of the Temperature Application to Four *n*-Alkanes ($C_{16}H_{34}$, $C_{18}H_{38}$, $C_{19}H_{40}$ and $C_{21}H_{44}$) under Saturating Vapour Pressure in the 298-573 K Range. Thermochim. Acta 2006, 445, 32-35.
31. Findenegg, G. H. Density and Coefficient of Expansion of Some Liquid Alkanes. Monatshefte fur Chemie 1970, 101, 1081-1088.
32. Finke, H. L.; Gross, M. E.; Waddington, G.; Huffman, H. M. Low-Temperature Thermal Data for the Nine Normal Paraffin Hydrocarbons from Octane to Hexadecane. J. Am. Chem. Soc. 1954, 76, 333-341.
33. Francis, F.; Wood, N. E. The Boiling Points of Some Higher Aliphatic *n*-Hydrocarbons. J. Chem. Soc. 1926, 129, 1420-1423.
34. Glaser, M.; Peters, C. J.; van der Kooi, H. J.; Lichtenthaler, R. N. Phase Equilibria of (Methane + *n*-Hexadecane) and ($p$, $V_m$, $T$) of *n*-Hexadecane. J. Chem. Thermodyn. 1985, 17, 803-815.
35. Gollis, M. H.; Belenyessy, L. I.; Gudzinowicz, B. J.; Koch, S. D.; Smith, J. O.; Wineman, R. J. Evaluation of Pure Hydrocarbons as Jet Fuels. J. Chem. Eng. Data 1962, 7, 311-316.
36. Gouel, P. Density of Alkanes ($C_6$ to $C_{16}$) Cyclics and Alkyl-Benzenes. Bull. Cent. Rech. Explor.-Prod. Elf-Aquitaine 1978, 2, 211-225.
37. Graaf, G. H.; Smit, H. J.; Stamhuis, E. J.; Beenackers, A. A. C. M. Gas-Liquid Solubilities of the Methanol Synthesis Components in Various Solvents. J. Chem. Eng. Data 1992, 37, 146-158.
38. Grenier-Loustalot, M. F.; Potin-Gautier, M.; Grenier, P. Analytical Applications of Measurements of Vapor Pressures During the Saturation of an Inert Gas with Normal Alkanes and Polyethylene Glycols. Analyt. Letters 1981, 14, 1335-1349.
39. Khasanshin, T. S.; Shchemelev, A. P. Sound Velocity in Liquid n-Alkanes. High Temp. 2001, 39, 60-67.
40. Krafft, F. Ueber Neunzehn Hohere Normalparaffine $C_nH_{2n+2}$ Und Ein Einfaches Volumgesetz Fur Den Tropfbar Flussigen Zustand. Ber. Dtsch. Chem. Ges. 1882, 15, 1687-1712.
41. Lainez, A.; Rodrigo, M.-M.; Wilhelm, E.; Grolier, J.-P. E. Excess Volumes and Excess Heat Capacities of Some Mixtures with trans, trans,cis-1,5,9-Cyclododecatriene at 298.15 K. J. Chem. Eng. Data 1989, 34, 332-335.
42. Lauer, J. L.; King, R. W. Refractive Index of Liquids at Elevated Temperatures. Anal. Chem. 1956, 28, 1967-1701.
43. Lee, C.-H.; Dempsey, D. M.; Mohamed, R. S.; Holder, G. D. Vapor-Liquid Equilibria in the Systems of *n*-Decane/Tetralin, *n*-Hexadecane/Tetralin, *n*-Decane/1-Methylnaphthalene and 1-Methylnaphthalene/Tetralin. J. Chem. Eng. Data 1992, 37, 183-186.
44. Matthews, M. A.; Rodden, J. B.; Akgerman, A. High-Temperature Diffusion, Viscosity, and Density Measurements in n-Hexadecane. J. Chem. Eng. Data 1987, 32, 317-319.
45. Melaugh, R. A.; Mansson, M.; Rossini, F. D. The Energy of Isomerization of *n*-Dodecane Into 2,2,4,6,6-Pentamethylheptane. J. Chem. Thermodyn. 1976, 8, 623-626.
46. Mills, P. L.; Fenton, R. L. Vapor Pressures, Liquid Densities, Liquid Heat Capacities, and Ideal Gas Thermodynamic Properties for 3-Methylhexanal and 3,4-Dimethylpentanal. J. Chem. Eng. Data 1987, 32, 266-273.
47. Morawetz, E. A Non-Equilibrium Low Vapor Pressure Heat of Vaporization Calorimeter. Acta Chem. Scand. 1968, 22, 1509-1531.
48. Morawetz, E. The Correlation of Enthalpies of Vaporization of Isomeric Alkanes with Molecular Structure. J. Chem. Thermodyn. 1972, 4, 145-151.
49. Morgan, D. L.; Kobayashi, R. Direct Vapor Pressure Measurements of Ten *n*-Alkanes in the $C_{10}$-$C_{28}$ Range. Fluid Phase Equilib. 1994, 97, 211-241.

50. Myers, H. S.; Fenske, M. R. Measurement and Correlation of Vapor Pressure Data for High Boiling Hydrocarbons. Ind. Eng. Chem. 1955, 47, 1652-1658.
51. Nascimento, F. P.; Melh, A.; Ribas, D. C.; Paredes, M. L. L.; Costa, A. L. H.; Pessoa, F. L. P. Experimental High Pressure Speed of Sound and Density of (Tetralin + *n*-Decane) and (Tetralin + *n*-Hexadecane) Systems and Thermodynamic Modeling. J. Chem. Thermodyn. 2015, 81, 77-88.
52. Neruchev, Y. A.; Bolotnikov, M. F.; Zotov, V. V. Investigation of Ultrasonic Velocity in Organic Liquids on the Saturation Curve. Thermochim. Teplofiz. Vys. Temp. 2005, 43, 274-316.
53. Neruchev, Y. A.; Zotov, V. V.; Otpushennikov, N. F. Speed of Sound and Adiabatic Compressibility of Some n-Paraffins. Ukr. Fiz. Zh. 1967, 12, 1385-1387.
54. Outcalt, S. L.; Laesecke, A.; Fortin, T. J. Density and speed of sound measurements of hexadecane. J. Chem. Thermodynamics 2010, 42, 700-706.
55. Paredes, M. L. L.; Reis, R. A.; Silva, A. A.; Santos, R. N. G.; Santos, G. J. Densities, Sound Velocities, and Refractive Indexes of Tetralin + *n*-Hexadecane at (293.15, 303.15, 313.15, 333.15, and 343.14) K. J. Chem. Eng. Data 2011, 11, 4076-4082.
56. Parks, G. S.; Moore, G. E. Vapor Pressure and Other Thermodynamic Data for n-Hexadecane and n-Dodecylcyclohexane near Room Temperature. J. Chem. Phys. 1949, 17, 1151-1153.
57. Peters, C.; Spiegelaar, J.; de Swaan Arons, J. Phase Equilibria in Binary Mixtures of Ethane + Docosane and Molar Volumes of Liquid Docosane. Fluid Phase Equilib. 1988, 41, 245-256.
58. Petit, J. C.; Ter Minassian, L. Measurements of (dV/dT)p (dV/dp)T, and (dH/dT)p by Flux Calorimetry. J. Chem. Thermodyn. 1974, 6, 1139-1152.
59. Piacente, V.; Fontana, D.; Scardala, P. Enthalpies of Vaporization of a Homologous Series of n-Alkanes Determined from Vapor Pressure Measurements. J. Chem. Eng. Data 1994, 39, 231-237.
60. Piacente, V.; Pompili, T.; Scardala, P. Temperature Dependence of the Vaporization Enthalpies of n-Alkanes from Vapour Pressure Measurements. J. Chem. Thermodyn. 1991, 23, 379-396.
61. Plantier, F.; Daridon, J.-L.; Lagourette, B.; Boned, C. Isentropic Thermophysical Properties of Pure n-Paraffins as a Function of Temperature and Chain Length. High Temp.-High Press. 2000, 32, 305-310.
62. Plebanski, T.; Wozniak, M.; Wilanowska, K. A Dilatometric Method for Measuring the Density of Organic Liquid at Elevated Temperatures. Nauchn. Apparat. 1986, 1, 47-59.
63. Prak, D. J. L.; Brown, E. K.; Trulove, P. C. Density, Viscosity, Speed of Sound, Bulk Modulus of Methyl Alkanes, and Hydrotreated Renewable Fuels. J. Chem. Eng. Data 2013, 58, 2065-2075.
64. Prak, D. J. L.; Morris, R. E.; Cowart, J. S.; McDaniel, A. M.; Trulove, P. C. Density, Viscosity, Speed of Sound, Bulk Modulus, Surface Tension, and Flash Point of Binary Mixtures of n-Hexadecane + Ethylbenzene or + Toluene at (293.15 to 373.15) K and 0.1 MPa. J. Chem. Eng. Data 2014, 59, 3571-3585.
65. Queimada, A. J.; Quinones-Cisneros, S. E.; Marrucho, I. M.; Coutinho, J. A. P.; Stenby, E. H. Viscosity and Liquid Density of Asymmetric Hydrocarbon Mixtures. J. Chem. Eng. Data 2003, 24, 1221-1239.
66. Queimada, A. J.; Marrucho, I. M.; Coutinho, J. A. P.; Stenby, E. H. Viscosity and Liquid Density of Asymmetric n-Alkane Mixtures: Measurements and Modeling. Int. J. Thermophys. 2005, 26, 47-61.
67. Sasse, K.; Jose, J.; Merlin, J.-C. A Static Apparatus for Measurement of Low Vapor Pressures. Experimental Results on High Molecular-Weight Hydrocarbons. Fluid Phase Equilib. 1988, 42, 287-304.
68. Schiessler, R. W.; Herr, C. H.; Rytina, A. W.; Weisel, C. A.; Fischl, F.; McLaughlin, R. L.; Kuehner, H. H. The Synthesis and Properties of Hydrocarbons of High Molecular Weight-IV. Proc. Am. Pet. Inst., Sect. 3, 1946, 26, 254-302.
69. Siitsman, C.; Kamenev, I.; Oja, V. Vapor Pressure Data of Nicotine, Anabasine and Cotinine Using Differential Scanning Calorimetry. Thermochim. Acta 2014, 595, 35-42.

70. Snyder, P. S.; Winnick, J. The Pressure, Volume and Temperature Properties of Liquid *n*-Alkanes at Elevated Pressures. Proc. 5th Symp. Thermophys. Prop. 1970, 5, 115-129.
71. Tanaka, Y.; Hosokawa, H.; Kubota, H.; Makita, T. Viscosity and Density of Binary Mixtures of Cyclohexane with *n*-Octane, *n*-Dodecane, and *n*-Hexadecane Under High Pressures. Int. J. Thermophys. 1991, 12, 245-264.
72. Tardajos, G.; Aicart, E.; Costas, M.; Patterson, D. Liquid Structure and Second-Order Mixing Functions for Benzene, Toluene and *p*-Xylene with n-Alkanes. J. Chem. Soc., Faraday Trans. 1, 1986, 82, 2977-2987.
73. Tardajos, G.; Diaz Pena, M.; Aicart, E. Speed of Sound in Pure Liquids by a Pulse-Echo-Overlap Method. J. Chem. Thermodyn. 1986, 18, 683-689.
74. Viton, C.; Chavret, M.; Behar, E.; Jose, J. Vapor Pressure of Normal Alkanes from Decane to Eicosane at Temperatures from 244 K to 469 K and Pressures from 0.4 Pa to 164 kPa. Int. Electron. J. Phys.-Chem. Data 1996, 2, 215-224.
75. Vogel, A. I. Physical Properties and Chemical Constitution. Part IX. Aliphatic Hydrocarbons. J. Chem. Soc. 1946, 146, 133-139.
76. Wilhelm, E.; Lainez, A.; Roux, A. H.; Grolier, J.-P. E. Excess Molar Volumes and Heat Capacities of (1,2,4-Trichlorobenzene+an *n*-Alkane) and (1-Chloronaphthalene + an *n*-Alkane). Thermochim. Acta 1986, 105, 101-110.
77. Wu, J.; Shan, Z.; Asfour, A.-F. A. Viscometric Properties of Multicomponent Liquid *n*-Alkane Systems. Fluid Phase Equilib. 1998, 143, 263-274.
78. Wu, Y.; Bamgbade, B.; Liu, K.; Hugh, M. A. M.; Baled, H. Experimental Measurements and Equation of State Modeling of Liquid Densities for Long-Chain n-Alkanes at Pressures to 265 MPa and Temperatures to 523 K. Fluid Phase Equilib. 2011, 311, 17-24.
79. Wuerflinger, A.; Mondieig, D.; Rajabalee, F.; Cuevas-Diarte, M. A. *pVT* Measurements and Related Studies on the Binary System $n C_{16}H_{34}$-$nC_{17}H_{36}$ and on $nC_{18}H_{38}$ at High Pressures. Z. Naturforsh A 2001, 56, 626-634.
80. Wuerflinger, A.; Sandmann, M. Thermodynamic Measurements on *n*-Hexadecane ($C_{16}H_{34}$) and *n*-Heptadecane ($C_{17}H_{36}$) at Elevated Pressures. Z. Naturforsh S 2000, 55, 533-538.
81. Young, S. On the Boiling Points of the Normal Paraffins at Different Pressures. Proc. R. Irish Acad. 1928, 38B, 65-92.
82. Zolghadr, A.; Escrochi, M.; Ayatollahi, S. Temperature and Composition Effect on $CO_2$ Miscibility by Interfacial Tension Measurement. J. Chem. Eng. Data 2013, 58, 3536-3544.
83. Zuiderweg, F. J. Vacuum Distillation I. Test Mixtures for Evaluation of Low Pressure Columns. Chem. Eng. Sci. 1952, 1, 164-174.
84. Diky, V.; Chirico, R. D.; Frenkel, M.; Bazyleva, A.; Magee, J. W.; Paulechka, E.; Kazakov, A. F.; Lemmon, E. W.; Muzny, C. D.; Smolyanitsky, A. Y.; Townsend, S.; Kroenlein, K. NIST Standard Reference Database 103b: Thermo Data Engine (TDE), Version 10.1; National Institute of Standards and Technology, Standard Reference Data Program, Gaithersburg, 2015.
85. Lemmon, E. W.; Goodwin, A. Critical Properties and Vapor Pressure Equation for Alkanes $C_nH_{2n+2}$: Normal Alkanes With $n \leq 36$ and Isomers for $n = 4$ Through $n = 9$. J. Phys. Chem. Ref. Data 2000, 29, 1–39.
86. Linstrom, P. J.; Mallard, W.G., Eds., NIST Chemistry WebBook, NIST Standard Reference Database Number 69, National Institute of Standards and Technology, Gaithersburg MD, 20899, https://doi.org/10.18434/T4D303 (retrieved May 16, 2022).
87. Wagner, W. A Method to Establish Equations of State Exactly Representing all Saturated State Variables Applied to Nitrogen. Cryogenics 1972, 12, 214-221.

88. Lemmon, E. W.; McLinden, M. O.; Wagner, W. Thermodynamic Properties of Propane. III. A Reference Equation of State for Temperatures from the Melting Line to 650 K and Pressures up to 1000 MPa. J. Chem. Eng. Data 2009, 54, 3141–3180.
89. Newell, D.B.; Cabiati, F.; Fischer, J.; Fujii, K.; Karshenboim, S.G.; Margolis, H.S.; de Mirandes, E.; Mohr, P.J.; Nez, F.; Pachucki, K.; *et al.* The CODATA 2017 values of *h*, *e*, *k*, and $N_A$ for the revision of the SI. Metrologia 2018, 55, L13–L16.
90. Span, R. Multiparameter Equations of State: An Accurate Source of Thermodynamic Property Data. Springer Science & Business Media, 2000.
91. Venkatarathnam, G.; Oellrich, L. Identification of the Phase of a Fluid using Partial Derivatives of Pressure, Volume, and Temperature without Reference to Saturation Properties: Applications in Phase Equilibria Calculations. Fluid Phase Equilib. 2011, 301, 225–233.
92. Lemmon, E.W.; Bell, I.H.; Huber, M.L.; McLinden, M.O. NIST Standard Reference Database 23: Reference Fluid Thermodynamic and Transport Properties-REFPROP, Version 10.0, National Institute of Standards and Technology, Standard Reference Data Program, Gaithersburg, 2018.
93. Thol, M.; Lemmon, E. W. Equation of State for the Thermodynamic Properties of trans-1,3,3,3-Tetrafluoropropene [R-1234ze(E)]. Int. J. Thermophys. 2016, 37, 1–16.
94. Zhou, Y.; Lemmon, E. W. Equation of State for the Thermodynamic Properties of 1,1,2,2,3-Pentafluoropropane (R-245ca). Int. J. Thermophys. 2016, 37, 1–11.
95. Lemmon, E. W.; Jacobsen, R. T. A New Functional Form and New Fitting Techniques for Equations of State with Application to Pentafluoroethane (HFC-125). J. Phys. Chem. Ref. Data 2005, 34, 69–108.
96. Span, R.; Beckmüller, R.; Hielscher, S.; Jäger, A.; Mickoleit, E.; Neumann, T.; Pohl, S.; Semrau, B.; Thol, M. TREND. Thermodynamic Reference and Engineering Data 5.0. Lehrstuhl für Thermodynamik, Ruhr-Universität Bochum, 2020.
97. Bell, I. H.; Wronski, J.; Quoilin, S.; Lemort, V. Ind. Eng. Chem. Res. 2014, 53, 2498.